

Original paper

Developing finite volume method (FVM) in numerical simulation of flow pattern in 60° open channel bend

Azadeh Gholami^{1,2}, Hossein Bonakdari^{1,2,*}, Ali Akbar Akhtari^{1,2}

¹Department of Civil Engineering, Razi University, Kermanshah, Iran.

²Water and Wastewater Research Center, Razi University, Kermanshah, Iran.

ARTICLE INFO

Article history:

Received 9 January 2016

Received in revised form 21 March 2016

Accepted 5 April 2016

Keywords:

Numerical simulation
Finite volume method (FVM)
Developed FLUENT software
60° bend

ABSTRACT

In meandering rivers, the flow behavior is very complex due to topography and flow depth changes. In general, effective forces on bend flow pattern include centrifugal force due to non-uniformity of the vertical velocity profile and radius pressure gradient induced by the lateral slope of water surface. In this paper, the 60° bend flow pattern is simulated by developing FLUENT computational software based on finite volume method (FVM), numerically. The $k-\epsilon$ (RNG) turbulence model and volume of fluid (VOF) method are used for turbulence and flow depth modeling. The FVM numerical results are verified by existing experimental data in velocity and flow depth. The results illustrate that the FVM model has high accuracy in prediction flow variables in the bend. As the average value of root mean square error (RMSE) and mean absolute percentage error (MAPE) values between the observational and numerical results for depth-averaged velocity (DAV) in the different transverse profile are 4.5 and 9%, respectively, which is an acceptable error percentage. The advanced software can well simulate the both major and minor secondary current cells with opposite rotation direction in the vicinity of channel bed and vicinity the water level in the outer wall, respectively. By the development of the major and minor secondary currents in sections located 40 (cm) after the bend, longitudinal velocity shift, and the high-velocity zone moves further to the outer wall (and the channel bed) in depth. Therefore, it can be said the developing FLUENT software can be utilized in practical cases in design and execution of curved channel.

© 2016 Razi University-All rights reserved.

1. Introduction

For Meandering Rivers, flow patterns are complex, so that flow mechanics has specific characteristics at bends, not observed within straight channels. Combining between field experiments, laboratory experiments, and numerical simulations is the most effective way to enhance flow knowledge and turbulence structure in curved channels. There have been extensive researches undertaken into the flow in bend channels and this research can be distributed into two types, experimental and Numerically studies; Leschziner and Rodi (1979) using a numerical model simulated the flow schema in the 180° sharp bend. They found that the longitudinal pressure gradient is the main factor of the maximum velocity component transmission into the outer wall at the final of the sharp bend while in the mild bends secondary current is the main factor of displacement. De Vriend and Geoldof (1983) did extensive studies on changing the water level and velocity experimentally and declared that in the beginning of the bend, the maximum velocity is located near the inner wall and transmitted to the outer wall in the final cross section. Bergs (1990) examined the flow and topographical changes of the bed in a laboratorial curved flume with trapezoidal cross section and mobile bed. The result demonstrates that the flow is spiral in the primary cross sections of the bend. Jung and Yoon (2000) investigated the flow velocity field in any kind of bend. They declared that in mild bend the maximum velocity is located at the inner wall and gradually transmitted to the outer wall from the internal cross section of the bend. Blanckaert and Graf (2004) examined the velocity component changes, boundary shear stress and bed

topography variation in curved flumed. Sui et al. (2006) measured the local scour at the 90° bend experimentally. They stated that the Froude number, the properties of protective wall and the size of bed particles have a high effect on the scour amount in the vicinity of channel bed. Naji et al. (2010) conducted vast experimental and numerical studies on flow properties at 90° mild bend. They declared that the maximum velocity is placed in the inner wall in half of the bend and is transferred to outer wall from the 45° cross section. Barbhuiya and Talukdar (2010) tested the 3D flow variables such velocity component, turbulent tension, shear stress and scour in different section at the 90° bend. Uddin and Rahman (2012) measured the velocity components in three directions by ADCP velocity meter and erosion in the channel bed in the river bend by experimental and numerical models. They compared the experimental and numerical model result and pointed to the good agreement between data. Liaghat et al. (2014) examined the flow hydraulic in a curved flume with variable width by SSIIM model. Ramamurthy et al. (2013) simulated three-dimensional flow properties at 90° sharp bend by different turbulence models associate with the numerical model. The researchers said that the RSM (Reynolds stress model) turbulence model and volumes of fluid method are in acceptable adaptation with experimental results. Vaghefi et al. (2014) analyzed the shear stress amount in the 180° sharp bend channel bed. In this bend, the maximum shear stress in channel bed is located at the 40° sections close to the inner wall. Gholami et al. (2014) studied the hydraulic of flow in 90° sharp curved channel experimentally and numerically. They stated that the maximum velocity till the final sections remains in the inner wall and is moved to the channel axis in the final cross sections.

Corresponding author Email: bonakdari@yahoo.com.

Ajeel Fenjan et al. (2016) modeled the flow variables in the 60° bend using computational fluid dynamic (CFD) and artificial neural network (ANN) soft computing model. They compared the numerical and ANN results with experimental data and with each other. Their results illustrate that the ANN model acts more accurately than CFD model with low error indices. Gholami et al. (2015 a, b and 2016 a, b) studied the flow hydraulic of sharp curved channels by different soft computing methods. They pointed to study complex bend flow type and presented noticeable results. In this study, the accuracy and application of the FLUENT software based on finite volume method (FVM) in prediction of total flow variables in 60° bend is evaluated. Vast experimental study was done by author to test the velocity and water surface depth (Akhtari et al. 2009). Also, the numerical simulation is done for predicting flow variables and the results are verified in comparison of available experimental data. Also, the advancing the numerical software is examined in the prediction of velocity contour and secondary cell development. The different statistical indices are used to examine model efficiency.

2. Experimental model

Experimental Model Akhtari (2009) measured the flow variables in a 60° sharp bend in the hydraulics laboratory of Ferdowsi University of Mashhad, Iran. Channel test was included of three parts: the straight inlet channel 360 cm before the point in which the bend begins, the curved channel, central radius of this channel (R_c) is 60.45 cm. The ratio of the bend central radius to the channel width is 1.5 (R_c/b) and since this ratio is lesser than 3, the under- study bend is considered a sharp bend. The straight outlet channel after the bend is 180 cm long. The cross sections of the intended flume are square-shaped with a width of 40.3 and a height of 40.3 cm. channel bed and walls are made of Plexiglas with rigid fix bed. Figs. 1 and 2 show the laboratorial and geometrical shape of the flume, respectively.

In this paper, the experiments were carried out on a discharge of 25.3 l/s. The Froude number and Reynolds number was 0.34 and 44705, respectively. The hydraulic characteristic is shown in Table 1.

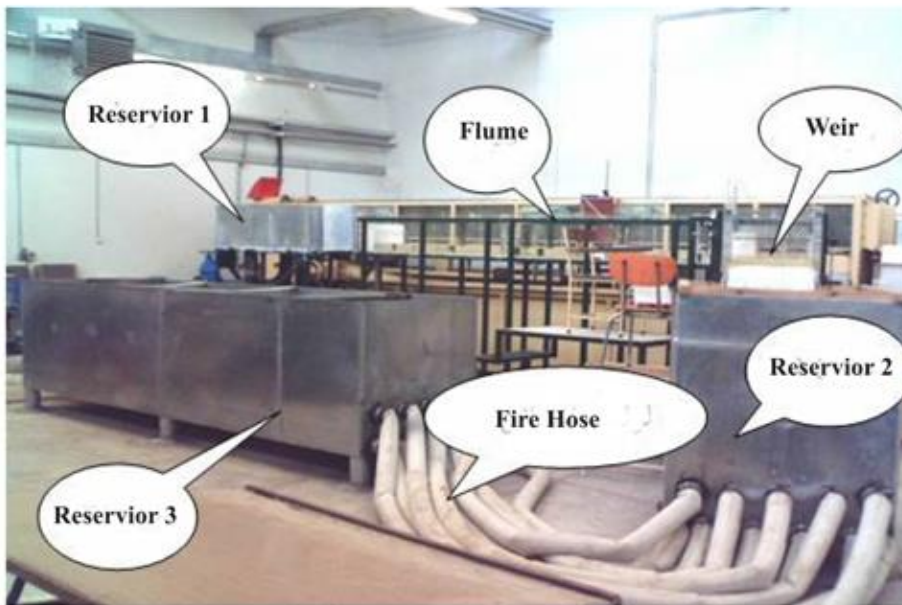


Fig. 1. The laboratorial flume of the 60° bend.

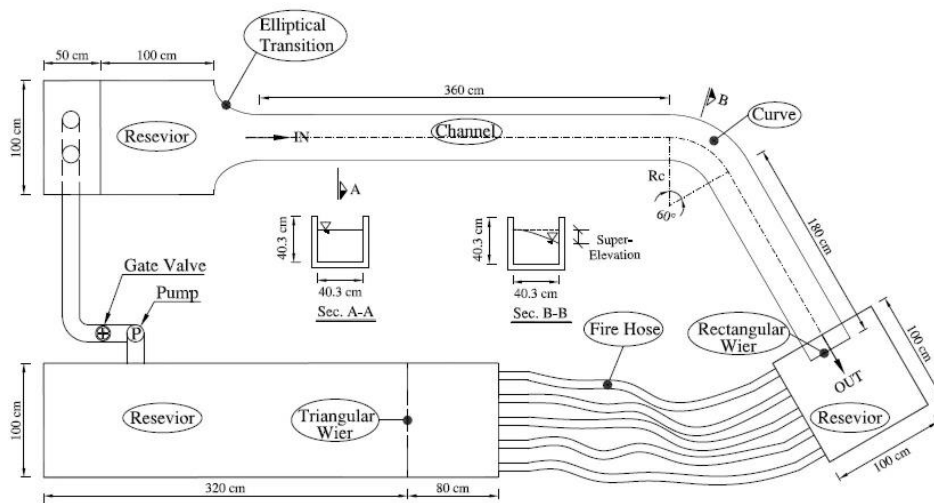


Fig. 2. The plan and geometry of the experimental flume related to the 60° bend.

Table 1. Hydraulic properties of test.

| Flow discharge Q (lit/s) | Flow depth Y (cm) | Flow velocity V (m/s) | Reynolds number | Froude number | Flow regime |
|--------------------------|-------------------|-----------------------|-----------------|---------------|---------------------------|
| 25.3 | 15 | 0.418 | 44705 | 0.34 | Turbulent and subcritical |

2.1. Numerical model

In this paper, the software Fluent was used for the numerical modeling. The software used the Finite Volume Method (FVM) for solving the flow equation (Manual. 2005). The FVM as a numerical method according to the integral conservation is utilized to compute the partial differential equations (e.g., Navier-Stokes equation) and then to calculate the flow variables values, averaged across the volume. The law of integral conservation is applied on small control volumes which are defined by the computational mesh.

2.2. The equations governing the flow

The equation governing the motion of a viscous in the compressible fluid at a turbulent state lays down down by average Navier-Stokes equations known as Reynolds (RANS). A state of the art CFD package; FLUENT, was employed to solve the governing equation, which used a finite volume method (FVM) to approximate the equations. The continuity equation (conservation of mass) and motion equation (momentum conservation) are stated as:

- Continuity equation

$$\frac{\partial \rho}{\partial t} + \frac{\partial}{\partial x_i} (\rho u_i) = 0 \tag{1}$$

- Momentum equation

$$\begin{aligned} &\frac{\partial}{\partial t} (\rho u_i) + \frac{\partial}{\partial x_i} (\rho u_i u_j) \\ &= -\frac{\partial P}{\partial x_i} + \frac{\partial}{\partial x_j} \left[\mu \left(\frac{\partial u_i}{\partial x_j} + \frac{\partial u_j}{\partial x_i} - \frac{2}{3} \delta_{ij} \frac{\partial u_l}{\partial x_l} \right) \right] \\ &+ \frac{\partial}{\partial x_j} (-\rho \overline{u_i' u_j'}) \end{aligned} \tag{2}$$

The k-ε (RNG) turbulence model as an exact and actuarial method and is utilized to the disjunction of Navier-Stokes equations.

In this paper, two methods are applied to determine the accuracy and suitability of the models. First, two relative and absolute error relations as the root mean square error (RMSE, Eq. (3)) and the mean absolute percentage error (MAPE, Eq. (4)) are used to evaluate model efficiency. Both are expressed in percentages and have an ideal value of zero.

$$RMSE = \left[\frac{\sum_{i=1}^N (Y_{i(actual)} - Y_{i(model)})^2}{N} \right]^{1/2} \times 100 \tag{3}$$

$$MAPE = \frac{1}{N} \sum_{i=1}^N \left(\frac{|Y_{i(actual)} - Y_{i(model)}|}{Y_{i(actual)}} \right) \times 100 \tag{4}$$

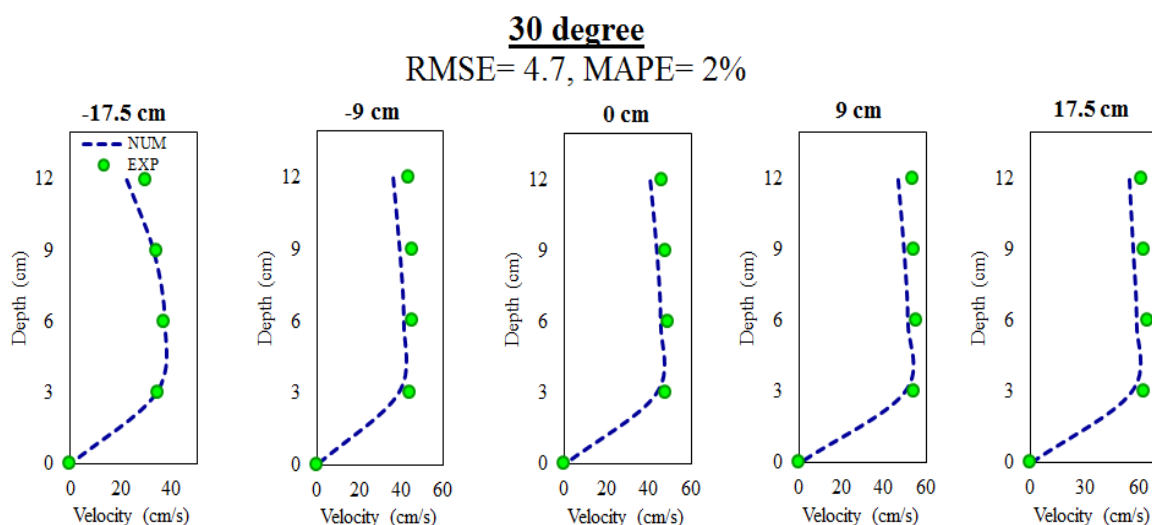
In this case, N is the number of measurement points, Y_{actual} is experimental measured data and Y_{model} is predicted by the model.

3. Results and discussion

3.1. Depth distribution of longitudinal velocity

In general, when flow approaches the bend, the secondary flow is generated gradually and causes the change in the velocity components at three directions x, y, z.

The maximum amount of the longitudinal velocity component is placed beneath the water surface and about the flow mid depth. In addition, the longitudinal velocity distribution is not logarithmic in the bend. In Fig. 3(a), (b), (c), and (d) show typical comparisons of the longitudinal computed and experimental velocity at 0°, 30°, 60° and 80 cm after bend cross sections, respectively. The mean difference (RMSE and MAPE errors) between the observational and FLUENT data have been shown in the top of the graphs. Fig 3 (b) which related to 30° bend section illustrates that the position of maximum velocity is close to the water surface. In Fig. 3 (c) the effect of secondary flow on the bend flow is noticeable at 60° section. In general, in sharp bends, by moving along the bend, the maximum velocity position is changed as it moves from the inner wall to the central channel axis and outer wall in the final cross sections of the bend. According to error values, it could be seen that the error values are acceptable. Relative error value in the 0° and 80 cm after the bend is more and less than the other cross section, respectively (1.53 % and 2.4 %). So, it can be said that model accuracy in the first and exit cross sections is high and low, respectively. Gholami et al. (2015a) Simulated hydraulic of bend flow using CFD and ANN models in 90° sharp bend. And their results represented that the CFD models can forecast flow hydraulic with no experimental data by RMSE of 2.33.



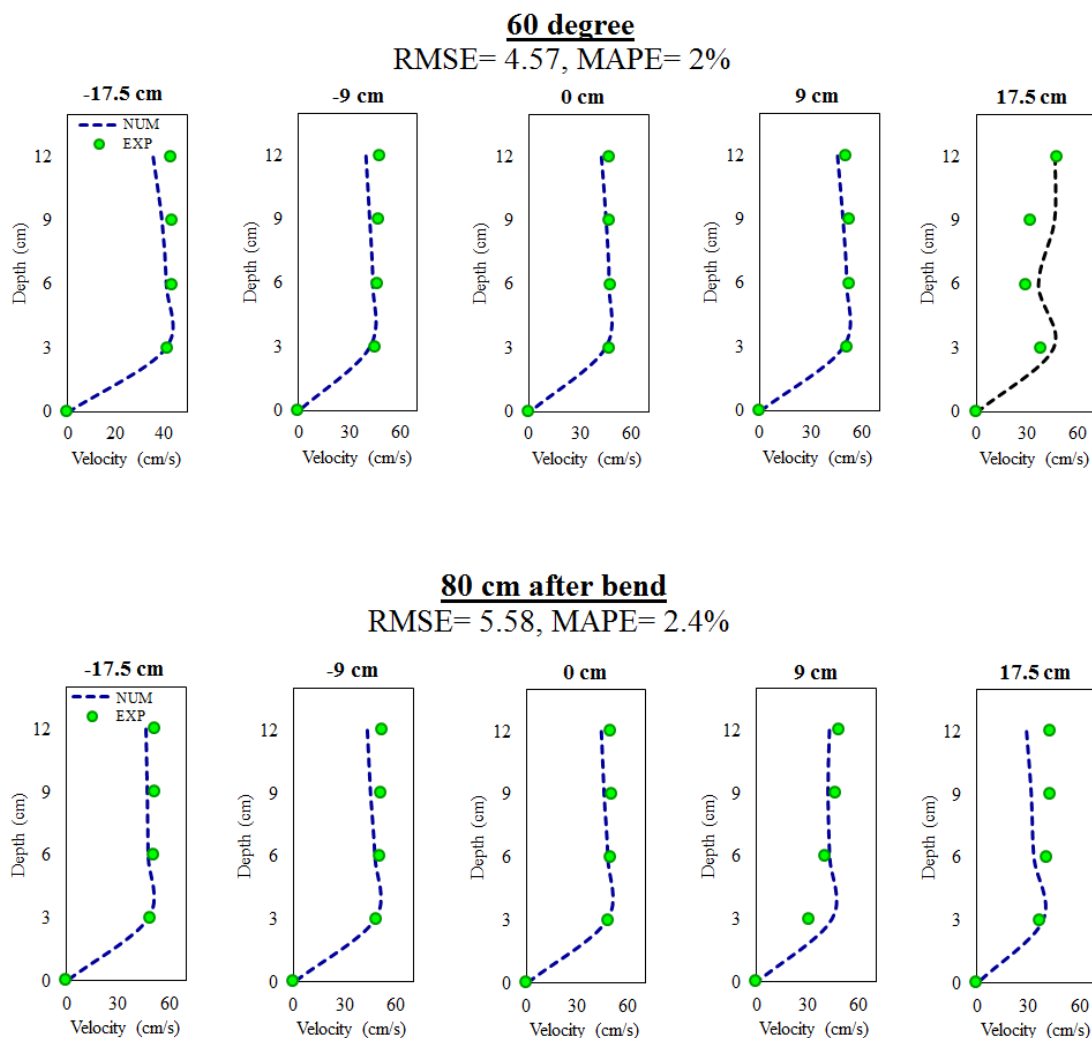


Fig. 3. Depth distributions of longitudinal velocity at cross sections of: (a) 0°, (b) 30°, (c) 60°, (d) 80 cm after bend.

Figs. 4 and 5 show the transverse profile of velocity predicted by numerical FLUENT model in comparison of observational values in different distance from the channel bed (Z= 3, 6, 9 and 12 cm from the channel bed) in 30° and 80 cm after the bend cross sections, respectively. The numerical simulation results match the experimental values with a great degree of compliancy. The RMSE and MAPE error values in Z= 3, 6, 9, and 12 (cm) and also the error values of the depth averaged velocity have been presented in Table 2 for all different cross sections.

The difference between the numerical and experimental results (RMSE) of the transversal distribution of axial velocities is at most approximately 16 % and the rest of these values range between 2 and 9 %. These error values are very much satisfactory. The lateral velocity profile represents the maximum level of inconsistency between the numerical and observational results at the input cross sections (40 cm before the bend and 0°) and the 50° and 60° cross sections especially in the layers near the channel bed which indicates that the numerical model is unable to suddenly increase the velocity and the flow undergoes separation in these cross sections (such Fig. 5).

Table 2. The RMSE and MAPE error values of velocity values predicted by numerical and experimental data at different cross sections, distance from the channel bed and averaged level.

| Cross sections | Z= 0.03 m | | Z= 0.06 m | | Z= 0.09 m | | Z= 0.12 m | | Average velocity | |
|----------------|-----------|-------|-----------|------|-----------|-------|-----------|-------|------------------|-------|
| | RMSE | MAPE | RMSE | MAPE | RMSE | MAPE | RMSE | MAPE | RMSE | MAPE |
| 40cm before | 2.34 | 4.73 | 3.08 | 6.00 | 4.27 | 8.22 | 6.24 | 12.69 | 3.96 | 7.88 |
| 0° | 2.52 | 9.54 | 2.90 | 5.56 | 4.65 | 8.78 | 6.03 | 11.94 | 3.97 | 7.81 |
| 10° | 4.66 | 9.54 | 4.46 | 8.06 | 4.71 | 8.60 | 6.69 | 13.72 | 5.04 | 9.95 |
| 20° | 4.34 | 8.93 | 3.75 | 6.91 | 5.14 | 9.84 | 6.44 | 13.61 | 4.81 | 9.74 |
| 30° | 4.84 | 9.37 | 4.03 | 7.19 | 5.17 | 9.84 | 6.83 | 14.55 | 5.12 | 10.14 |
| 40° | 4.64 | 8.69 | 3.72 | 6.89 | 5.27 | 10.54 | 9.78 | 16.35 | 4.97 | 10.06 |
| 50° | 3.19 | 6.11 | 2.57 | 5.08 | 4.43 | 8.76 | 6.81 | 13.78 | 4.03 | 8.29 |
| 60° | 3.04 | 5.78 | 2.78 | 5.50 | 5.56 | 10.64 | 6.97 | 13.27 | 4.13 | 8.52 |
| 40 cm after | 5.79 | 12.17 | 2.90 | 6.10 | 6.91 | 13.20 | 7.67 | 15.06 | 4.04 | 8.07 |
| 80 cm after | 5.15 | 9.45 | 4.18 | 8.08 | 7.85 | 15.01 | 8.38 | 16.11 | 4.96 | 9.12 |

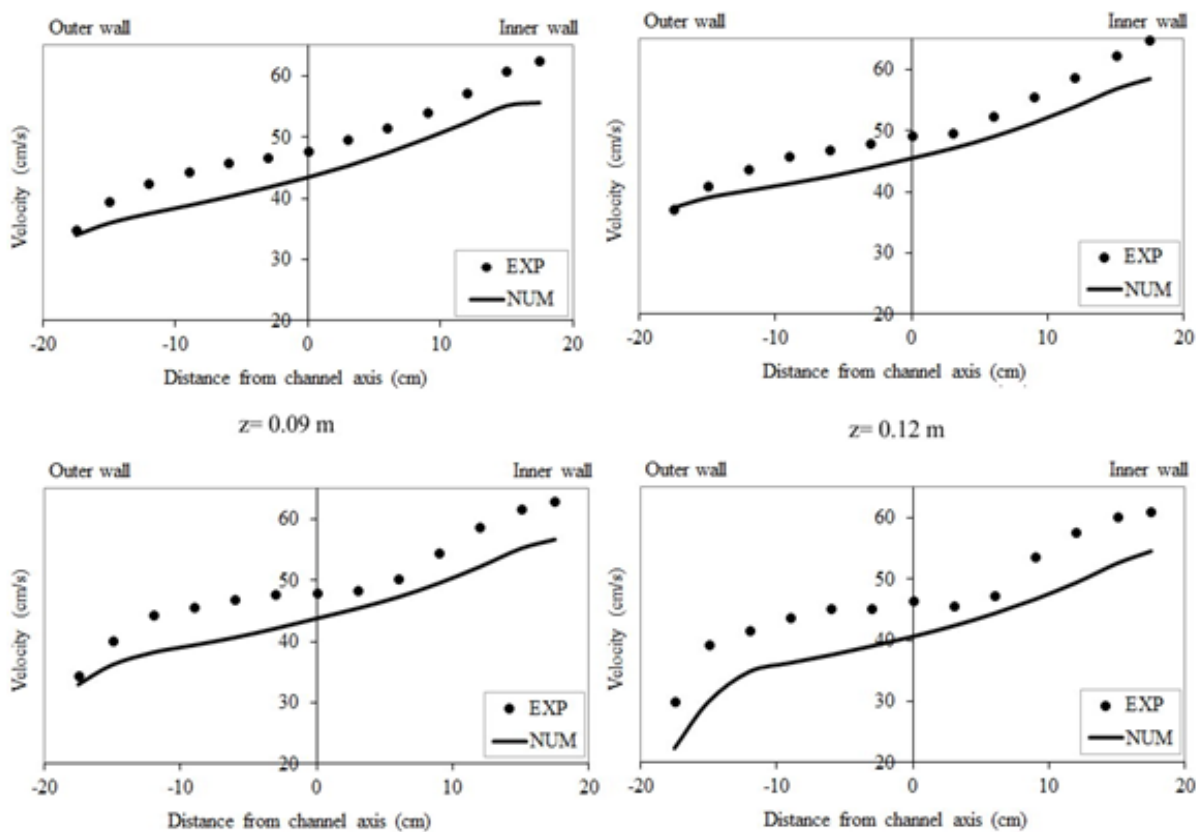


Fig. 4. The experimental and numerical results comparison of the lateral velocity distribution in the 30° cross section at the different distance from the channel bed ($z = 0.03, 0.06, 0.09,$ and 0.12 m).

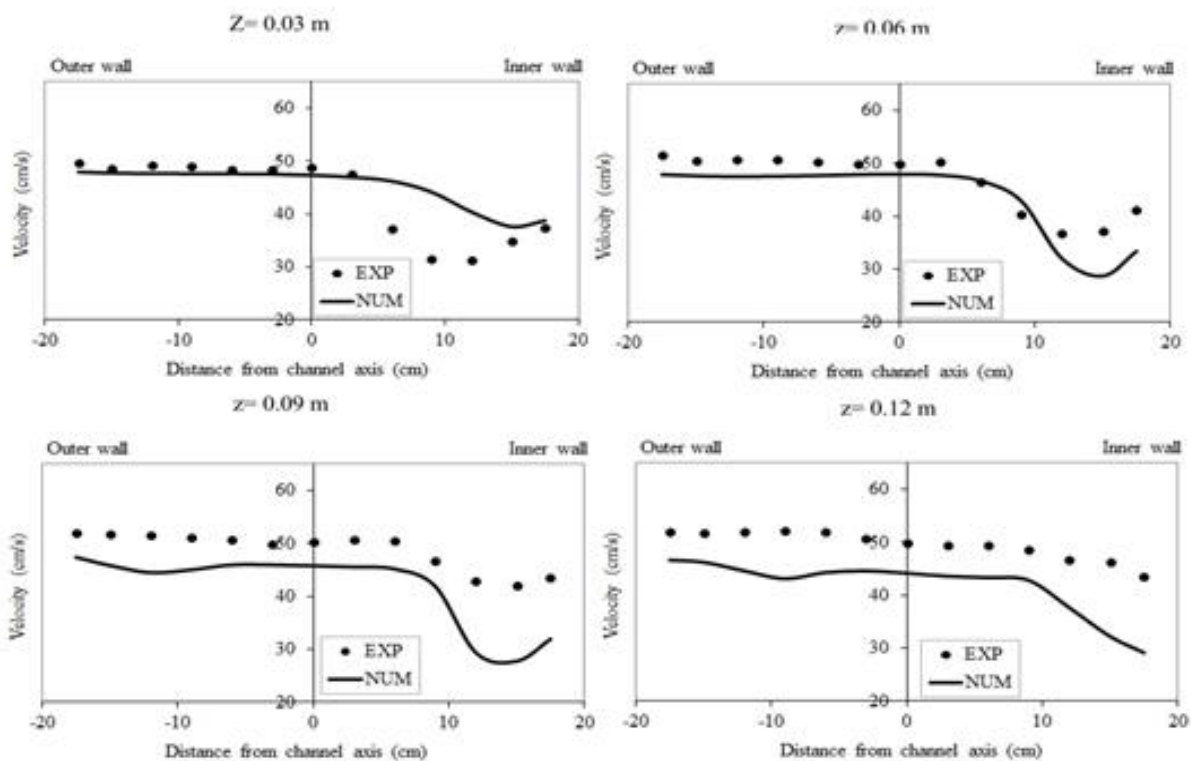


Fig. 5. The experimental and numerical results comparison of the lateral velocity distribution in the cross section of 80 cm after the bend at the different distance from the channel bed ($z = 0.03, 0.06, 0.09,$ and 0.12 m).

3.3. Longitudinal distribution of flow depth

Fig. 6 shows the numerical results of longitudinal flow depth distribution through the inner wall, the axis, and the channel outer wall in comparison with the corresponding experimental values. The values of RMSE and MAPE between these results have been presented in Table 3. The figure and the values make it clear that the fairly consistent results along with 0.12 and 0.61 % respectively for RMSE and MAPE

mean values through the bend are acceptable. MAPE error value in the outer wall is higher than another longitudinal axis (1.03 %). The increase in the water level before the bend in order to gain the required energy to enter the bend could be clearly seen in both the experimental and numerical models. Therefore, it can be said that the numerical model enables to untangle the governing equation into the flow type in bends and has high accuracy in flow variables prediction.

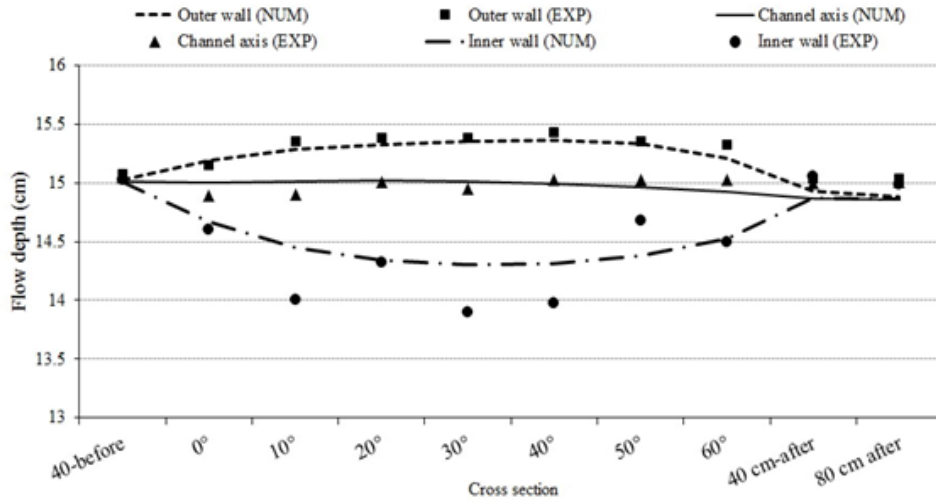


Fig. 6. Comparing the longitudinal distribution of the flow depth in the inner wall, the channel axis, and the outer wall in experimental and numerical models.

Table 3. RMSE and MAPE values between the flow depth values in the experimental and the numerical models through the channel length.

| Channel length | RMSE | MAPE (%) |
|----------------|-------|----------|
| Outer wall | 0.22 | 1.03 |
| Channel axis | 0.081 | 0.42 |
| Outer wall | 0.07 | 0.37 |
| Mean RMSE | 0.12 | 0.61 |

3.4. Velocity contours prediction

Fig. 7 shows three dimensional contours of the velocity magnitude in different cross section of 0°, 10°, 20°, 30°, 40°, 50°, 60°, 40 and 80

cm after the bend. When flow enters the bend, the maximum velocity zone locates in the inner wall. This trend continues up to the other sections. Since the presented 60° bend is sharp, the maximum velocity takes place in the inner wall and reminds in this wall.

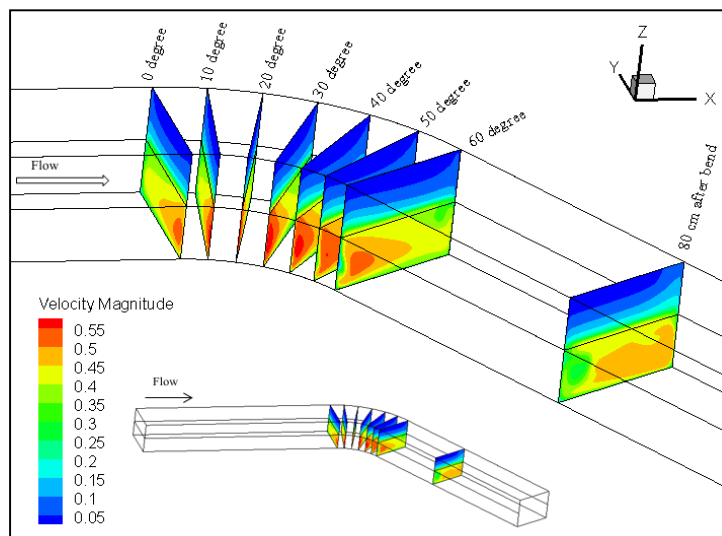


Fig. 7. Longitudinal velocity contours at different sections of 0°, 10°, 20°, 30°, 40°, 50°, 60°, and cross sections located 40 and 80 cm after the bend.

By moving along the bend, the secondary flow is generated which is important hydraulic phenomena in bend channels. By the enlargement of the major and minor secondary flows, it can be seen that in the section located 40 cm after the bend longitudinal velocity shifts and the high-velocity zone moves further to the outer wall and the bed of channel. And at the section of 80 cm after the bend, the high-velocity zone is completely separated from the inner wall and transfers to the outer wall.

3.5. Secondary currents cells simulation

Fig. 8 shows the secondary flow at the different cross sections. As seen, at the bend entrance section (0°) a one-way radial flow towards the inner wall is seen which is caused by the longitudinal pressure gradient created in the bend. In the later cross sections, the secondary

flow is produced and continued up till the cross section after the bend. As seen in figures, at all sections, the rotation of the major secondary flow with clockwise rotation direction is seen. The center of the major secondary flow transfers from the outer wall towards the inner wall by advancing along the bend. In this state, the major secondary flow causes a surface flow to be pushed to the outer wall; this flow comes up after disorienting with the outer wall, and then goes back towards the inner wall. This process causes another secondary flow cell to be formed in the outer wall and close to the water surface, which is called the minor secondary flow and its rotation direction is contrary to the major secondary flow. Therefore, at a 60° sharp bend, the minor secondary flow begins from the angle of 20° and continues to some distances following the bend. By going through the bend in the cross sections located after the bend, both cell secondary flows decrease because of the weakness of their power.

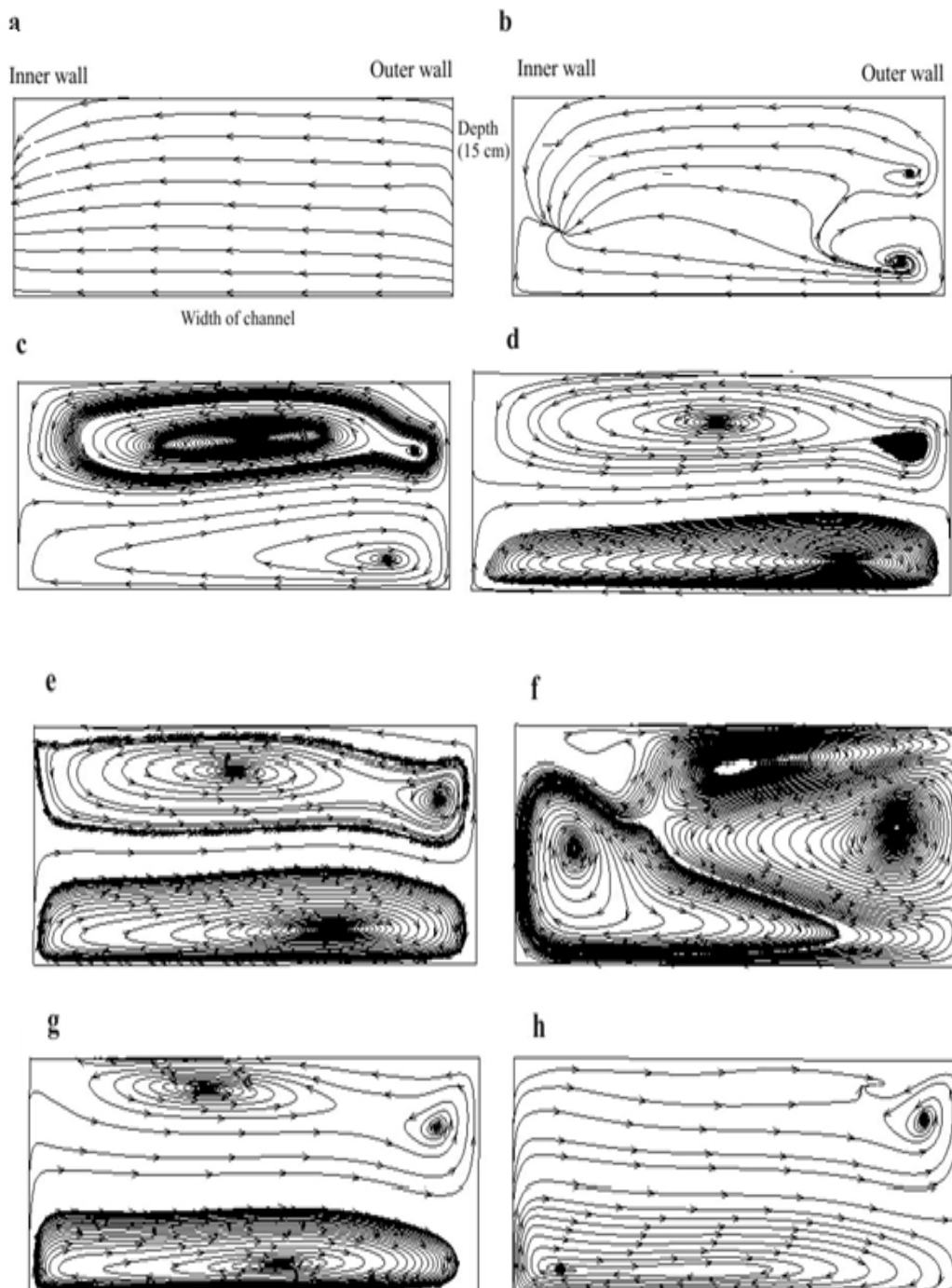


Fig. 8. The secondary flows at different sections: (a) 0°, (b) 10°, (c) 20°, (d) 30°, (e) 40°, (f) 50°, (g) 60°, (h) 80 cm after the bend cross section.

4. Conclusions

In this paper, the application of numerical software is evaluated through flow hydraulic in a curved channel. The used numerical model is based on finite volume method (FVM) that can simulate the complicated flow pattern in bends. The results illustrate that the FVM model has high accuracy in prediction of flow variables and also can well predict the powerful secondary current cells that this cell simulation is so difficult sometimes (Naji Abhari et al. 2010). The important results show that:

1. In the sharp bends, the maximum velocity through the exit bend cross sections are located in the inner wall and later with the advent and the growth of the secondary flow is moved to the channel axis and in the section after the bend in the outer wall occurs.
2. The error values of velocity component between numerical and observational data are more (1.53 %) and less (2.4 %) than the other cross section at the section of 0° and 80 cm after the bend, respectively.

So, it can be said the model accuracy in the first and exit cross sections is high and low, respectively.

3. The MAPE, when comparing the longitudinal distribution of the flow depth in the inner wall, the channel axis, and the outer wall in experimental and numerical models was acceptable and in the outer wall is higher than another longitudinal axis (1.03 %).
4. The fairly consistent results along with 0.12 and 0.61 % for RMSE values through the bend are acceptable.
5. The FLUENT software simulates the major and minor secondary cell as well as other flow variables in channel width and outer wall, respectively.
6. The proposed numerical model can well predict the high and low velocity zones and subsequently the erosion and sedimentation place in sharp bends.

References

- Akhtari A.A., Abrishami J., Sharifi M.B., Experimental investigations water surface characteristics in strongly-curved open channels, *Journal of Applied Sciences* 9 (2009) 3699-3706.
- Barbhuiya A. K., Talukdar S., Scour and three dimensional turbulent flow fields measured by ADV at a 90degree horizontal forced bend in a rectangular channel, *Flow Measurement and Instrumentation* 21(2010) 312-321.
- Bergs M. A., Flow processes in a curved alluvial channel, PhD Dissertation, Iowa University (1990).
- Blanckaert K., Graf W. H., Momentum transport in sharp open-channel bends, *Journal of Hydraulic Engineering* 130 (2004) 186-198.
- De Vriend H. J., Geldof H.J., Main flow velocity in short river bends, *Journal of Hydraulic Engineering* 109 (1983) 991-1011.
- Fenjan S.A., Bonakdari H., Gholami A., Akhtari A.A., Flow variables prediction using experimental, computational fluid dynamic and artificial neural network models in a sharp bend, *International Journal of Engineering-Transactions A: Basics* 29 (2016) 14-22.
- Gholami A., Akhtari A. A., Minatour Y., Bonakdari H., Javadi A. A., Experimental and numerical study on velocity fields and water surface profile in a strongly-curved 90° open channel bend, *Engineering Applications of Computational Fluid Mechanics* 8 (2014) 447-461.
- Gholami A., Bonakdari H., Zaji A.H., Ajeel Fenjan S., Akhtari A.A., Design of modified structure multi-layer perceptron networks based on decision trees for the prediction of flow parameters in 90° open-channel bends, *Engineering Applications of Computational Fluid Mechanics* 10 (2016a)194-209.
- Gholami A., Bonakdari H., Zaji A. H., Akhtari A.A., Simulation of open channel bend characteristics using computational fluid dynamics and artificial neural networks, *Engineering Applications of Computational Fluid Mechanics* 9 (2015a) 355-369.
- Gholami A., Bonakdari H., Zaji A.H., Akhtari A.A., Khodashenas S.R., Predicting the velocity field in a 90° open channel bend using a genetic expression programming model, *Flow Measurement and Instrumentation* 46 (2015b) 189-192.
- Gholami A., Bonakdari H., Zaji A.H., Michelson D.G., Akhtari A. A., Improving the performance of multi-layer perceptron and radial basis function models with a decision tree model to predict flow variables in a sharp 90° bend, *Applied Soft Computing* 48 (2016b) 563-583.
- Jung J. W., Yoon S. E., Flow and bed topography in a 180-degree curved channel, In 4th international conference on hydro-science and engineering, Korea Water Resources (2000) Association.
- Leschziner M. A., Rodi W., Calculation of strongly curved open channel flow, *Journal of the Hydraulics Division* 105 (1979) 1297-1314.
- Liaghat A., Mohammadi K., Rahmanshahi M., 3D Investigation of Flow Hydraulic in U Shape Meander Bendswith Constant, Decreasing and Increasing Width, *Journal of river engineering* 2 (2014) 12-23.
- Manual, Fluent, Manual and user guide of Fluent Software, Fluent Inc, (2005).
- Naji Abhari M., Ghodsian M., Vaghefi M., Panahpur N., Experimental and numerical simulation of flow in a 90° bend, *Flow Measurement and Instrumentation* 21 (2010) 292-298.
- Ramamurthy A., Han S., Biron P., Three-Dimensional simulation parameters for 90° open channel bend flows, *Journal of Computing in Civil Engineering- ASCA* 27 (2013) 282-291.
- Sui J., Fang D., Karney B.W., An experimental study into local scour in a channel caused by a 90 bend, *Canadian Journal of Civil Engineering* 33 (2006) 902-911.
- Uddin M. N., Rahman M.M., Flow and erosion at a bend in the braided Jamuna River, *International Journal of Sediment Research* 27 (2012) 498-509.
- Vaghefi M., Akbari M., Fiouz A.R., Experimental Investigation on Bed Shear Stress Distribution in a 180 Degree Sharp Bend by using Depth-Averaged Method, *International Journal of Scientific Engineering and Technology* 3 (2014) 962-966.